

C.P. No. 424

(18,735)

A.R.C. Technical Report

C.P. No. 424

(18,735)

A.R.C. Technical Report



MINISTRY OF SUPPLY

AERONAUTICAL RESEARCH COUNCIL

CURRENT PAPERS

The Interaction between a Weak Normal Shock Wave and a Turbulent Boundary Layer

*G. E. Gadd, Ph.D.,
of the Aerodynamics Division, N.P.L.*

LONDON: HER MAJESTY'S STATIONERY OFFICE

1959

Price 4s. 6d. net

The Interaction between a Weak Normal Shock Wave
and a Turbulent Boundary Layer

- By -

G. E. Gadd, Ph.D.
of the Aerodynamics Division, N.P.L.

19th June, 1957

SUMMARY

A theory is presented for the interaction between a weak normal shock in an initially uniform mainstream, and an idealised boundary layer, with frictionless, one-dimensional, subsonic flow, on a flat wall. Reasons are given for believing that, despite the drastic simplifications of the model, it is not altogether unreal. Hence it is hoped that the results will prove helpful in interpreting experimental findings for real turbulent layers.

In the theory, the flow is assumed to take place in a two-dimensional channel. For such flow, the final downstream pressure depends on the ratio of the boundary layer thickness to the height of the channel, and on the upstream Mach number M_0 , which is assumed to be in the range 1 to 1.1. Theoretical estimates are given for the downstream pressure, and by a slight extension, they may be applied to the case of flow through a circular pipe. The theory also predicts the shape of the pressure distribution at the wall, and its mode of variation with Mach number M_0 and with channel height or pipe diameter.

1. Introduction

In, for example, transonic flow past aerofoils, nearly-normal shock waves occur and interact with the boundary layer. When the local free-stream Mach number just upstream of the shock exceeds about 1.2,¹ separation is provoked even when, as in most practical cases, the boundary layer is turbulent. However, with the thin aerofoil sections now coming into use, local supersonic Mach numbers between, say, 1 and 1.15 are quite commonly encountered just ahead of the shock when the angle of incidence is small. Shocks at such Mach numbers do not provoke separation of the turbulent boundary layer, but even so it is usually found¹ that the pressure rise experienced at the surface of the aerofoil underneath the shock wave is appreciably less than what may be termed the full theoretical normal-shock value. The latter is the pressure rise which would occur for a normal shock in inviscid flow in a duct of constant cross-sectional area with a uniform upstream Mach number equal to the local Mach number at the edge of the boundary layer upstream of the shock on the aerofoil. The theoretical pressure rise is not attained partly because of the finite nature of the supersonic region and the consequent decrease of Mach number with increasing distance from the surface just upstream of the shock^{2,3}. Even, however, when the surface is locally flat, so that the rate of change of upstream Mach number with distance from the surface is zero at the wall, local pressure rises considerably less than the theoretical normal-shock values are often observed⁴. The reason is that the boundary layer thickens under the shock wave, so that just outside the boundary layer the stream-tube areas are reduced downstream, with a consequent reduction in pressure.

These/

These effects of boundary-layer thickening, which will always be present even when the effects of the finite nature of the supersonic region are also important, could be studied in isolation in a suitable experiment. Thus a pipe could be used, with air flowing through it at a Mach number a little above 1 initially, and dropping to below 1 through a normal shock. If the radius of the pipe were extremely large compared with the thickness of the boundary layer, the theoretical normal-shock pressure would be attained everywhere across the pipe sufficiently far downstream. For more moderate ratios of pipe radius to boundary-layer thickness, the asymptotic downstream pressure would be somewhat less than the full theoretical value. In all cases, however, it is likely that the pressure distribution at the wall would depart from the theoretical discontinuous jump in pressure that would occur in the absence of a boundary layer, and instead would exhibit a spreading out proportional to boundary-layer thickness. Also, the pressure immediately under the shock might possibly rise only to a value considerably lower than the final value, which might not be reached until many boundary-layer thicknesses downstream of the shock.

The present paper gives a very approximate theory for the conditions of the above hypothetical experiment, except that, for simplicity, the flow is considered as being in a straight two-dimensional channel instead of the experimentally more convenient pipe. It is hoped that the paper will throw light on the effects associated with nearly-normal shock waves on aerofoils in transonic flow, insofar as these effects are concerned with boundary-layer thickening rather than with the curvature of the surface and the corresponding non-uniformity of the upstream flow. Hence the slightly supersonic mainstream is assumed to be initially uniform and the wall to be flat. The problem is simplified by treating the boundary layer as if it were a uniform subsonic frictionless layer of initial upstream Mach number M_{S0} and thickness t_0 , as in Fig.1. The initial free-stream Mach number is M_0 , a little greater than 1. This model of the flow is the same as that used by Tsien and Finston⁵, but the analysis is different because the equations of motion in the external flow cannot be linearised in the same way for Mach numbers near 1 as they can for larger Mach numbers. Furthermore, the external flow is subsonic downstream of the shock in the present case.

It might be thought to be a retrogressive step to adopt the inviscid model used by Tsien and Finston, in the light of more recent theories (e.g., Ref.6) which take account of viscosity. However in the special case of a turbulent boundary layer with a free stream Mach number near 1, the neglect of viscous and turbulent friction is probably not a fatal defect. Fig.2 shows the shape of the real velocity profile both at an upstream position and also downstream, after the boundary layer has met with an adverse pressure gradient. The profile in the laminar sublayer must distort as shown, so that the friction stress increases with distance away from the wall, thus balancing the pressure gradient. Hence the laminar sublayer will experience a large proportional increase in thickness. Friction plays an essential part here, because in the absence of friction the slowest-moving fluid would immediately be brought to rest by the slightest pressure increase. However for the more rapidly moving fluid, friction is not so important. All the subsonic stream tubes in the boundary layer will expand on encountering increases of pressure, but where the velocity is relatively high, this expansion will largely be due to the inviscid "Bernouilli" effect. Since in a turbulent boundary layer with a free-stream Mach number near 1 a large fraction of the boundary layer is subsonic, and the laminar sublayer is very thin compared with this subsonic region, the thickening of the sublayer will not be a dominant factor, though it may well be important. Also, although friction may play a significant rôle in the more rapidly moving parts of the layer, the frictionless "Bernouilli" effect here is likely to be the most important one, and the present model which considers only this factor and ignores effects of friction will not be completely unreal. It is not, of course, to be expected that the results of the analysis will be quantitatively exact for the real case, but it is hoped that they will give a useful qualitative picture of what happens.

In view of the crudity of the assumption that friction can be neglected, it seems inappropriate to attempt a complicated analysis if further simplifications can be made. This is the reason why the form shown in Fig.1 has been chosen for the idealised boundary-layer profile, since it is in any case necessary to assume that there is a non-zero slip velocity at the wall. For otherwise, if a realistic boundary layer velocity profile were assumed with the flow frictionless, the fluid immediately adjacent to the wall would be unable to withstand any pressure increase.

In the interests of simplicity again, the flow in the subsonic layer is treated as one-dimensional, i.e., the pressure and velocity are treated as constant across the layer, and dependent only on the distance x along the wall. This probably introduces only small errors since the inclination of the flow to the wall is everywhere small, and the solution obtained involves no discontinuities of slope at the edge of the layer.

As mentioned above, the case considered in the analysis is that of the flow in a two-dimensional channel. The overall flow pattern for the interaction between the shock and the subsonic layers on the two walls of the channel is as shown in Fig.3. The centre line is of course a line of symmetry so that only one half of the channel need be considered. In the external flow near the edge of the subsonic layer there will be a band of compression waves which will be terminated downstream by the shock wave. The solution for the compression-wave region upstream of the shock is comparatively easy to obtain, but the flow downstream of the shock presents a difficult problem. This is partly because the boundary conditions at the edge of the subsonic layer and just behind the shock are complicated. The shock boundary conditions, in particular, depend on the shape of the shock, which in turn is affected by the downstream flow. When the height of the channel is limited, so that the final downstream pressure differs appreciably from the full normal-shock value, it turns out to be easier to obtain a formal solution for the downstream flow than when the channel is infinite. However the accurate evaluation of the downstream solution for the finite channel is impracticably tedious, and a crude approximation is accordingly made to it.

Section 3 presents the somewhat lengthy analysis resulting in what is, granted the basic assumptions, the almost exact solution for the flow upstream of the shock, and the very rough solution for the downstream flow, and the relevance of all this to the real case is discussed in Sections 4 and 5.

2. List of Symbols

x	distance measured parallel to the wall, measured from the point at which the shock intersects the subsonic layer
y	distance measured normal to the wall
s	distance along a streamline
n	distance normal to a streamline
ψ	stream function defined by Equation (17), and the condition $\psi = 0$ at the edge of the subsonic layer
\bar{x}	equal to Nx , where N is given by Equation (37)
$\bar{\psi}$	equal to $N\psi$, where N is given by Equation (37)
C	value of ψ on the centre line of the channel
y_C	distance of the centre line of the channel from the wall
t	thickness of the subsonic layer

δ	total thickness of the real turbulent boundary layer upstream of the region of interaction
Y	thickness of the subsonic part of the real turbulent boundary layer upstream of the region of interaction
X	x of the shock
\bar{X}	NX , where N is given by Equation (37)
θ	angle between the shock and the normal to the flow just upstream of it, or between the shock and the normal to the wall
ϵ	deflection angle of the flow on passing through the shock
α	inclination of the flow to the wall
q	total velocity
u	velocity component in the x direction
v	velocity component in the y direction
p	pressure
ρ	density
I	enthalpy
M	Mach number
γ	ratio of specific heats
k	related to pressure by Equation (8)
k_F	final downstream value of k
l	defined by Equation (21)
m	defined by Equation (22)
A	constant in the approximate relation (34) for the thickness of the subsonic layer
N	defined by Equation (37)
S	defined by Equation (46)
F	ratio t_0/Y
suffix S	refers to conditions in the subsonic layer
suffix 0	refers to conditions upstream of the region of interaction
suffix S0	refers to conditions in the subsonic layer upstream of the region of interaction
suffix 1	refers to conditions just upstream of the shock
suffix 2	refers to conditions just downstream of the shock

3. Analysis

3.1 Characteristics of the shock wave

Consider an oblique shock inclined at an angle θ to the normal to the flow just upstream of it, as in Fig.4. Let quantities just upstream of the shock be distinguished by suffix 1. In the central part of the channel these upstream quantities will take their undisturbed free-stream values, denoted by suffix 0, but near the walls the shock will occur as the termination of a compression-wave region, as shown in Fig.3, and hence here the flow conditions just upstream of the shock will differ from those in the free stream. If quantities just downstream of the shock are distinguished by suffix 2, we have:-

$$\text{Energy:} \quad \frac{\gamma}{\gamma-1} \frac{p_2}{\rho_2} + \frac{q_2^2}{2} = \frac{\gamma}{\gamma-1} \frac{p_1}{\rho_1} + \frac{q_1^2}{2} \quad \dots(1)$$

Momentum parallel to bc in Fig.4:

$$p_2 - p_1 = \rho_1 q_1 (q_1 - q_2 \cos \epsilon), \quad \dots(2)$$

where ϵ is the angle of deflection of the flow on passing through the shock.

Momentum parallel to ac in Fig.4:

$$q_2 \sin (\theta + \epsilon) = q_1 \sin \theta,$$

$$\text{or} \quad \tan \theta = - \frac{q_2 \sin \epsilon}{q_2 \cos \epsilon - q_1} \quad \dots(3)$$

$$\text{Continuity:} \quad \rho_2 q_2 \cos (\theta + \epsilon) = \rho_1 q_1 \cos \theta,$$

$$\text{or} \quad \tan \theta = \frac{\rho_2 q_2 \cos \epsilon - \rho_1 q_1}{\rho_2 q_2 \sin \epsilon} \quad \dots(4)$$

From (3) and (4),

$$\rho_2 = \frac{\rho_1 q_1 (q_1 - q_2 \cos \epsilon)}{q_2 (q_1 \cos \epsilon - q_2)}$$

$$\text{But from (2)} \quad q_2 = \left[q_1 - \frac{p_2 - p_1}{\rho_1 q_1} \right] \sec \epsilon, \quad \dots(5)$$

$$\text{so that} \quad \rho_2 = \frac{(p_2 - p_1) \cos^2 \epsilon}{\left[\frac{p_2 - p_1}{\rho_1 q_1} - q_1 \sin^2 \epsilon \right] \left[q_1 - \frac{p_2 - p_1}{\rho_1 q_1} \right]} \quad \dots(6)$$

Hence, /

Hence, in (1)
$$\frac{\gamma}{\gamma-1} p_2 \left[\frac{p_2-p_1}{\rho_1 q_1} - q_1 \sin^2 \epsilon \right] \left[q_1 - \frac{p_2-p_1}{\rho_1 q_1} \right] \frac{\sec^2 \epsilon}{p_2-p_1} + \frac{1}{2} \left[q_1 - \frac{p_2-p_1}{\rho_1 q_1} \right]^2 \sec^2 \epsilon = \frac{\gamma}{\gamma-1} \frac{p_1}{\rho_1} + \frac{q_1^2}{2},$$

or
$$\sin^2 \epsilon \left\{ \frac{\gamma p_1}{(\gamma-1)(p_2-p_1)} + \frac{\gamma+1}{2(\gamma-1)} - \frac{\gamma(p_2-p_1)}{(\gamma-1)\rho_1 q_1^2} - \frac{2\gamma p_1}{(\gamma-1)\rho_1 q_1^2} \right\} = \frac{(p_2-p_1)}{(\gamma-1)\rho_1 q_1^2} \left[1 - \frac{\gamma p_1}{\rho_1 q_1^2} - \frac{(\gamma+1)(p_2-p_1)}{2\rho_1 q_1^2} \right]. \quad \dots(7)$$

Put
$$\frac{p}{p_0} = 1 + \frac{2\gamma}{\gamma+1} (M_0^2 - 1)(1 - k), \quad \dots(8)$$

so that when $k = 0$ the pressure takes the value that it has just behind a normal shock with upstream Mach number M_0 . Throughout the external flow-field, the Mach number M is related to the enthalpy I by the relation:

$$I \left(1 + \frac{\gamma-1}{2} M^2 \right) = I_0 \left(1 + \frac{\gamma-1}{2} M_0^2 \right).$$

Hence
$$M^2 - 1 = \frac{\gamma+1}{\gamma-1} \left(\frac{I_0}{I} - 1 \right) + \frac{I_0}{I} (M_0^2 - 1).$$

Upstream of the shock the flow is isentropic and

$$\frac{I_0}{I} = \left(\frac{p}{p_0} \right)^{-\frac{(\gamma-1)}{\gamma}}$$

Thus from (8)
$$\frac{I_0}{I} \approx 1 - \frac{2(\gamma-1)}{\gamma+1} (1 - k)(M_0^2 - 1)$$

if M_0 is close to 1, and

$$M^2 - 1 = (2k - 1)(M_0^2 - 1) \quad \dots(9)$$

in the external flow upstream of the shock*. From (8) it follows that

$$\frac{p_2-p_1}{p_1} \approx \frac{2\gamma}{\gamma+1} (k_1 - k_2)(M_0^2 - 1),$$

and hence Equation (7) reduces approximately to

$$\epsilon = \frac{2(M_0^2-1)^{\frac{3}{2}}}{(\gamma+1) M_0^2} (k_1 + k_2 - 1)^{\frac{1}{2}} (k_1 - k_2). \quad \dots(10)$$

This approximation is quite good even if M_0 is not very close to 1. Thus for example if $k_1 = 1$, the errors in (10) arise mainly from those terms in the bracketed expression on the left hand side of (7) which are neglected in deriving (10). The omitted terms are equal to

γ+1/

*Relation (9) is, in fact, approximately valid everywhere in the external flow.

$$\frac{\gamma+1}{2(\gamma-1)} - \frac{(p_2-p_1)}{(\gamma-1)p_1 M_1^2} - \frac{2}{(\gamma-1)M_1^2},$$

and partially cancel one another.

An expression for the angle θ between the shock and the normal to the flow just upstream of it can be obtained from Equations (3) and (5). Approximately

$$\theta = - \frac{q_2 \epsilon}{q_2 \cos \epsilon - q_1} \simeq \frac{\rho_1 q_1^2 \epsilon}{p_2 - p_1} \simeq \frac{\gamma p_1 M_0^2 \epsilon}{p_2 - p_1} = \frac{(\gamma+1)M_0^2 \epsilon}{2(k_1 - k_2)(M_0^2 - 1)}.$$

Hence from (10) $\theta = (M_0^2 - 1)^{\frac{1}{2}} (k_1 + k_2 - 1)^{\frac{1}{2}} \dots(11)$

This is approximately the angle between the shock and the normal to the wall, since, as is shown later, the angle between the flow just upstream of the shock and the wall is, like ϵ in Equation (10), of order $(M_0^2 - 1)^{\frac{3}{2}}$.

The configuration of the shock wave shown in Fig.3 is in accordance with relation (11). At the centre of the channel the shock must be normal and θ zero by symmetry. Provided the height of the channel is sufficient, the flow upstream of the shock will be outside the compression-wave region, so that $k_1 = k_0 = 1$. Hence $k_2 = 0$, i.e., the full normal-shock pressure is attained just downstream of the shock on the centre line. However the final pressure far downstream will be less than this, unless the height of the channel is infinite. At the junction with the subsonic layer there can be no abrupt change of flow angle or discontinuity in pressure at the shock wave, and this condition is satisfied if the compression-wave region extends as far as a local external Mach number of 1 with $k_1 = k_2 = \frac{1}{2}$. [See Equations (9) and (10).] Hence the shock, which is here of zero strength, is again normal to the wall. At points between the centre line and the junction with the subsonic layer, k_1 will be between 1 and $\frac{1}{2}$, and k_2 between $\frac{1}{2}$ and 0. Probably $k_1 + k_2$ will be greater than 1 - it cannot be less than 1 by (10) - hence the shock will be inclined as shown in Fig.3.

3.2 The relation between pressure and flow angle in the compression-wave region

It is assumed that the compression-wave region is of the simple-wave type. This means that Mach waves emanating from adjacent points at the outer edge of the subsonic layer must, as shown in Fig.3, intersect and be terminated by the shock wave before they intersect each other. This assumption cannot be conclusively checked without knowing the complete solution to the problem, since the form of the shock wave is affected by conditions downstream. However according to the solution obtained in a later section for the flow upstream of $x = 0$, (the line defined, as in Fig.3, by the points at which the shock intersects the edges of the subsonic layers), the Mach waves are a long way from intersecting each other on $x = 0$, and although the shock is some distance to the right of this line, it seems likely that the waves will still not have intersected each other before they reach it. This justifies the simple-wave assumption, according to which the angle between the flow and the wall can be determined from the pressure, as follows:-

Fig.5 shows a short length ac of a streamline in the simple-wave region. The line ab is a Mach line, so that k is constant along ab , and bc is normal to ac . The angle abc is $\tan^{-1} (M^2 - 1)^{\frac{1}{2}} \simeq \tan^{-1} [(2k - 1)^{\frac{1}{2}} (M_0^2 - 1)^{\frac{1}{2}}]$ by Equation (9). Hence if n represents distance along the normal and s distance along the streamline,

$$\begin{aligned} \frac{\partial k}{\partial n} &= \frac{k_b - k_c}{bc} = \frac{k_a - k_c}{bc} = \frac{(k_a - k_c)}{ac} (2k-1)^{\frac{1}{2}} (M_0^2 - 1)^{\frac{1}{2}} \\ &= -(2k-1)^{\frac{1}{2}} (M_0^2 - 1)^{\frac{1}{2}} \frac{\partial k}{\partial s}. \end{aligned}$$

The pressure gradient normal to the streamlines balances the centrifugal force associated with the streamline curvature. Thus if the angle of the streamline to the wall is α ,

$$\frac{\partial p}{\partial n} = -\rho q^2 \frac{\partial \alpha}{\partial s} \simeq -\gamma p_0 M_0^2 \frac{\partial \alpha}{\partial s}.$$

But
$$\frac{\partial p}{\partial n} = -\frac{2\gamma p_0}{\gamma+1} (M_0^2 - 1) \frac{\partial k}{\partial n} \text{ by (8).}$$

Hence
$$\frac{\partial \alpha}{\partial s} = \frac{2(M_0^2 - 1)}{(\gamma+1)M_0^2} \frac{\partial k}{\partial n} = -\frac{2(M_0^2 - 1)^{\frac{3}{2}}}{(\gamma+1)M_0^2} (2k-1)^{\frac{1}{2}} \frac{\partial k}{\partial s}$$

and
$$\alpha = \frac{2(M_0^2 - 1)^{\frac{3}{2}}}{3(\gamma+1)M_0^2} [1 - (2k-1)^{\frac{3}{2}}], \quad \dots(12)$$

since $\alpha = 0$ when $k = 1$, in the undisturbed free stream. In (12), $1 \geq k \geq \frac{1}{2}$, since the flow must be supersonic in the simple wave region. [c.f. (9).] For this range of k there is not much difference between (12) and relation (10) for ϵ , the deflection angle through the shock, if in (10) we put $k_1 = 1$ and $k_2 = k$. These values for k_1 and k_2 would mean that the flow reached the pressure corresponding to k abruptly through a shock, with no region of gradual compression; the flow angle in these circumstances would, however, be little different at the low Mach numbers considered here from the flow angle produced by a continuous simple-wave compression to the same pressure.

3.3 The equation for the external flow downstream of the shock

The equations for the external flow are, in the usual notation,

$$\rho u \frac{\partial u}{\partial x} + \rho v \frac{\partial u}{\partial y} = -\frac{\partial p}{\partial x}, \quad \dots(13)$$

$$\rho u \frac{\partial v}{\partial x} + \rho v \frac{\partial v}{\partial y} = -\frac{\partial p}{\partial y}, \quad \dots(14)$$

$$\frac{\partial(\rho u)}{\partial x} + \frac{\partial(\rho v)}{\partial y} = 0, \quad \dots(15)$$

and
$$\frac{\gamma}{\gamma-1} \frac{p}{\rho} + \frac{(u^2 + v^2)}{2} = \frac{\gamma}{\gamma-1} \frac{p_0}{\rho_0} + \frac{u_0^2}{2}, \quad \dots(16)$$

where suffix 0 denotes initial upstream conditions.

Let/

Let a stream function ψ be defined by the relations

$$\rho u = \frac{\rho_0 u_0}{(M_0^2 - 1)^{\frac{1}{2}}} \left(\frac{\partial \psi}{\partial y} \right)_x, \quad \dots (17)$$

and

$$\rho v = - \frac{\rho_0 u_0}{(M_0^2 - 1)^{\frac{1}{2}}} \left(\frac{\partial \psi}{\partial x} \right)_y,$$

and the condition that $\psi = 0$ at the junction between the external flow and the subsonic layer. Equations (13) to (15) can be written in terms of x and ψ as independent variables, as follows:-

$$\rho u \left(\frac{\partial u}{\partial x} \right)_\psi = - \left(\frac{\partial p}{\partial x} \right)_\psi + (M_0^2 - 1)^{\frac{1}{2}} \frac{\rho v}{\rho_0 u_0} \left(\frac{\partial p}{\partial \psi} \right)_x \quad \dots (18)$$

$$\left(\frac{\partial v}{\partial x} \right)_\psi = - \frac{(M_0^2 - 1)^{\frac{1}{2}}}{\rho_0 u_0} \left(\frac{\partial p}{\partial \psi} \right)_x \quad \dots (19)$$

$$\text{and} \left[\frac{\partial(\rho u)}{\partial x} \right]_\psi - (M_0^2 - 1)^{\frac{1}{2}} \frac{\rho v}{\rho_0 u_0} \left[\frac{\partial(\rho u)}{\partial \psi} \right]_x + (M_0^2 - 1)^{\frac{1}{2}} \frac{\rho u}{\rho_0 u_0} \left[\frac{\partial(\rho v)}{\partial \psi} \right]_x = 0 \dots (20)$$

$$\text{As before we put} \quad \frac{p}{p_0} = 1 + \frac{2\gamma}{\gamma+1} (M_0^2 - 1)(1 - k). \quad \dots (8)$$

$$\text{We also put} \quad \frac{u}{u_0} = 1 + (M_0^2 - 1)\epsilon \quad \dots (21)$$

$$\text{and} \quad \frac{v}{u_0} = (M_0^2 - 1)^{\frac{3}{2}} m, \quad \dots (22)$$

since the proportional variation in u/u_0 will be of the same order as that in p/p_0 , and v/u_0 , which is approximately the angle between the flow direction and the wall, must be of the same order as ϵ and α in Equations (10) and (12). Equation (19) becomes

$$\left(\frac{\partial m}{\partial x} \right)_\psi = \frac{2}{(\gamma+1)M_0^2} \left(\frac{\partial k}{\partial \psi} \right)_x. \quad \dots (23)$$

The equation, similar to (13) and (14), relating the total velocity $q = (u^2 + v^2)^{\frac{1}{2}}$ to the variation of pressure with distance s along a streamline is

$$\rho q \frac{\partial q}{\partial s} = - \frac{\partial p}{\partial s},$$

and it follows from (16) that p/ρ^γ is constant along any streamline downstream of the shock. Strictly speaking, p/ρ^γ varies from streamline to streamline since the shock is curved, but this variation can be neglected since, at Mach numbers near to 1, p/ρ^γ downstream of a shock differs from its upstream value, p_0/ρ_0^γ , only by a term of order $(M_0^2 - 1)^3$. Hence from (8)

when $(2k - 1)^{\frac{1}{2}}$ is real, i.e., when $k \geq \frac{1}{2}$ and the flow is supersonic; downstream of the shock the solution takes a different form discussed in a later section.

3.4 The conditions imposed by the shock

If conditions just upstream and downstream of the shock are denoted by suffices 1 and 2 respectively, and α denotes the angle between the flow direction and the wall, then $\alpha_2 = \epsilon + \alpha_1$, where ϵ is given by (10) and α_1 is given by (12) with k put equal to k_1 . Thus

$$m_2 \simeq \frac{2}{(\gamma+1)M_0^2} \left\{ \frac{1}{3} [1 - (2k_1 - 1)^{\frac{3}{2}}] + (k_1 + k_2 - 1)^{\frac{1}{2}} (k_1 - k_2) \right\}, \quad \dots(29)$$

since from (22), m is approximately $(M_0^2 - 1)^{-\frac{3}{2}}$ times the flow angle. If x at the shock is denoted by X , it follows from (11) and (17) that approximately

$$\frac{dX}{d\psi} = (k_1 + k_2 - 1)^{\frac{1}{2}}. \quad \dots(30)$$

This relation determines k_2 , the value of k immediately downstream of the shock, in terms of the unknown, but in principle determinable, relation between X and ψ . Thus, as has already been mentioned, (30) implies that $k_2 = 0$ on the centre line of the channel, where $k_1 = 1$ and $dX/d\psi = 0$. In general, k upstream of the shock can be determined as a function of x and ψ , as will be shown in a later section. Hence k_1 is given for a given form of shock, and (30) then gives k_2 . Similarly (29) imposes conditions on k downstream of the shock. Thus consider for example conditions near the centre of the channel, where $k_1 = 1$. Relation (29) simplifies to

$$m_2 = \frac{2}{(\gamma+1)M_0^2} (1 - k_2)k_2^{\frac{1}{2}}.$$

$$\begin{aligned} \text{Hence } \frac{dm_2}{d\psi} &= \frac{2}{(\gamma+1)M_0^2} \frac{(1-3k_2)}{2k_2^{\frac{1}{2}}} \frac{dk_2}{d\psi} \\ &= \frac{2}{(\gamma+1)M_0^2} \frac{(1-3k_2)}{2k_2^{\frac{1}{2}}} \left[\left(\frac{\partial k}{\partial \psi} \right)_2 + k_2^{\frac{1}{2}} \left(\frac{\partial k}{\partial x} \right)_2 \right] \end{aligned}$$

by (30). Similarly

$$\begin{aligned} \frac{dm_2}{d\psi} &= \left(\frac{\partial m}{\partial \psi} \right)_2 + k_2^{\frac{1}{2}} \left(\frac{\partial m}{\partial x} \right)_2 \\ &= \frac{2}{(\gamma+1)M_0^2} \left\{ - (1 - 2k_2) \left(\frac{\partial k}{\partial x} \right)_2 + k_2^{\frac{1}{2}} \left(\frac{\partial k}{\partial \psi} \right)_2 \right\} \end{aligned}$$

by (23) and (26). Hence

$$\frac{(1-5k_2)}{k_2^{\frac{1}{2}}} \left(\frac{\partial k}{\partial \psi} \right)_2 + (3 - 7k_2) \left(\frac{\partial k}{\partial x} \right)_2 = 0. \quad \dots(31)$$

But/

But
$$\frac{d^2 X}{d\psi^2} = \frac{1}{2k_2^{\frac{1}{2}}} \frac{dk_2}{d\psi} \quad \text{by (30)}$$

$$= \frac{1}{2k_2^{\frac{1}{2}}} \left(\frac{\partial k}{\partial \psi} \right)_2 + \frac{1}{2} \left(\frac{\partial k}{\partial x} \right)_2.$$

Hence
$$(1 - 5k_2) \frac{d^2 X}{d\psi^2} + (1 - k_2) \left(\frac{\partial k}{\partial x} \right)_2 = 0. \quad \dots(32)$$

For any given form of the shock, relations (31) and (32) determine the first derivatives of k just behind the shock in the central part of the channel, and similar, but more complicated, relations can be obtained for the region nearer the wall where $k_1 \neq 1$.

3.5 The conditions imposed by the subsonic layer and the solution upstream of the shock

The pressure and other flow parameters in the subsonic layer are assumed to be constant across the layer and to be functions only of x . This assumption is probably fairly accurate since the streamline forming the boundary with the external flow is continuous everywhere in its slope, which is everywhere small. Denote by suffix S conditions in the subsonic layer, the additional suffix 0 being added to distinguish initial upstream values. Then

$$\frac{p_S}{p_{SO}} = \frac{p_S}{p_0} = 1 + \frac{2\gamma}{\gamma+1} (M_0^2 - 1)(1 - k_S) \quad \text{by (8),}$$

$$= \left[1 + \left(1 - \frac{u_S^2}{u_{SO}^2} \right) \frac{\gamma-1}{2} M_{SO}^2 \right]^{\frac{\gamma}{\gamma-1}}$$

by Bernoulli's equation. Also

$$\frac{\rho_S}{\rho_{SO}} = \left(\frac{p_S}{p_0} \right)^{\frac{1}{\gamma}} = \left[1 + \frac{2\gamma}{\gamma+1} (M_0^2 - 1)(1 - k_S) \right]^{\frac{1}{\gamma}}.$$

Hence if the thickness of the subsonic layer is t ,

$$\frac{t}{t_0} = \frac{\rho_{SO} u_{SO}}{\rho_S u_S} \quad \text{by continuity}$$

$$= \left(\frac{p_S}{p_0} \right)^{\frac{1}{\gamma}} \left[1 - \frac{2}{(\gamma-1)M_{SO}^2} \left\{ \left(\frac{p_S}{p_0} \right)^{\frac{\gamma-1}{\gamma}} - 1 \right\} \right]^{-\frac{1}{2}}. \quad \dots(33)$$

If M_0 is extremely close to 1, or if k is close to 1, (33) approximates to

$$\frac{t}{t_0} = 1 + \frac{2(M_0^2 - 1)(1 - M_{SO}^2)}{(\gamma+1)M_{SO}^2} (1 - k_S),$$

but this becomes very inaccurate for small values of k_S at Mach numbers M_0 above about 1.03. It is preferable, therefore, to use an approximate relation of the form

$$\frac{t}{t_0} = 1 + \frac{2(M_0^2 - 1)(1 - M_{SO}^2)}{(\gamma+1)M_{SO}^2} [1 - k_S + A(1 - k_S)^2], \quad \dots(34)$$

where/

where the constant A is chosen to give agreement with the more complicated exact form (33) at $k_S = 0$. Values of A thus determined are given in the attached Table.

TABLE 1

M_0		1	1.02	1.04	1.06	1.08	1.10
A for $M_{SO} = 0.6$	0	0.185	0.47	0.73	1.72	4.40	
	0.7	0.160	0.36	0.62	0.98	1.56	
	0.8	0.170	0.34	0.56	0.83	1.18	
	0.9	0.201	0.52	0.80	1.12	1.50	

Provided A is not too great, the approximation (34) represents the accurate form (33) quite well over the whole range $1 \geq k_S \geq 0$, as can be seen for the following calculated example, for $M_0 = 1.10$, $M_{SO} = 0.8$ and $A = 1.18$.

TABLE 2

k_S		0	0.2	0.4	0.6	0.8	1.0
t/t_0 according to (33)		1.215	1.146	1.093	1.054	1.023	1
t/t_0 according to (34)		1.215	1.153	1.101	1.058	1.024	1

From (34)

$$\frac{dt}{dx} = - \frac{2(M_0^2 - 1)(1 - M_{SO}^2)t_0}{(\gamma + 1)M_{SO}^2} [1 + 2A(1 - k_S)] \frac{dk_S}{dx} \quad \dots(35)$$

This is equal to the angle between the wall and the streamline $\psi = 0$, which forms the boundary between the external flow and the subsonic layer. On this streamline $k = k_S$, and it follows from Equation (12) that upstream of the shock

$$[1 + 2A(1 - k_S)] \frac{dk_S}{dx} + \frac{N}{3} [1 - (2k_S - 1)^{\frac{3}{2}}] = 0 \quad \dots(36)$$

where
$$N \equiv \frac{M_{SO}^2(M_0^2 - 1)^{\frac{1}{2}}}{M_0^2(1 - M_{SO}^2)t_0} \quad \dots(37)$$

Equation (36) can easily be integrated numerically for k_S in terms of Nx . Values are given in the attached Table for various values of A.

TABLE 3

k_S		0.5	0.6	0.7	0.8	0.9	0.95
$-Nx$ for A = 0	0	0.312	0.673	1.143	1.893	2.614	
	0.4	0.434	0.886	1.447	2.287	3.049	
	0.8	0.536	1.098	1.754	2.678	3.482	
	1.2	0.648	1.311	2.059	3.071	3.917	

The solution for k_S , equal to k along the streamline $\psi = 0$, determines k everywhere else in the external flow upstream of the shock. This is because k is constant along the Mach lines, which are inclined at an angle $\tan^{-1} [(2k - 1)^{\frac{1}{2}} (M_0^2 - 1)^{\frac{1}{2}}]$ to the normal to the wall. (Compare section 3.2.)

At $\psi = 0$ it follows from (22) that

$$\frac{dt}{dx} = (M_0^2 - 1)^{\frac{3}{2}} m.$$

Hence at $\psi = 0$,

$$\begin{aligned} (M_0^2 - 1)^{\frac{3}{2}} \frac{\partial m}{\partial x} &= \frac{2(M_0^2 - 1)^{\frac{3}{2}}}{(\gamma + 1)M_0^2} \frac{\partial k}{\partial \psi} \quad \text{by (23)} \\ &= - \frac{2(M_0^2 - 1)(1 - M_{SO}^2)t_0}{(\gamma + 1)M_{SO}^2} \left\{ [1 + 2A(1 - k_S)] \frac{d^2 k_S}{dx^2} - 2A \left(\frac{dk_S}{dx} \right)^2 \right\} \end{aligned}$$

by (35). Hence

$$[1 + 2A(1 - k)] \frac{\partial^2 k}{\partial x^2} - 2A \left(\frac{\partial k}{\partial x} \right)^2 + N \frac{\partial k}{\partial \psi} = 0 \quad \text{at } \psi = 0, \dots (38)$$

by (37). This relation applies both upstream and downstream of the shock, but it is only required as a boundary condition for the downstream flow.

From (36) it can be seen that at $\psi = 0$

$$\begin{aligned} \frac{\partial}{\partial x} \left\{ [1 + 2A(1 - k)] \frac{\partial k}{\partial x} \right\} &= [1 + 2A(1 - k)] \frac{\partial^2 k}{\partial x^2} - 2A \left(\frac{\partial k}{\partial x} \right)^2 \\ &\rightarrow 0 \quad \text{as } k \rightarrow \frac{1}{2}, \text{ i.e., as } x \rightarrow 0. \end{aligned}$$

Thus from (38) $\partial k / \partial \psi = 0$ at $x = \psi = 0$. From the equation of motion (27), $\frac{\partial^2 k}{\partial \psi^2} = 2 \left(\frac{\partial k}{\partial x} \right)^2$ at $x = \psi = 0$, where $k = \frac{1}{2}$.

Thus $\partial^2 k / \partial \psi^2$ is non-zero and positive whilst $\partial k / \partial \psi = 0$. However, downstream of the shock k cannot become greater than $\frac{1}{2}$, because it is assumed that the flow is subsonic. Hence there is a singularity immediately downstream of $x = \psi = 0$, implying an infinite negative value of $\partial^3 k / \partial \psi^3$. This singularity is, however, due only to the approximations made in the analysis. Really at $x = \psi = 0$ the gradient of k is zero in a direction locally normal to the streamline $\psi = 0$, rather than normal to the wall. Hence, since the streamline $\psi = 0$ is inclined at an angle $\frac{2(M_0^2 - 1)^{\frac{1}{2}}}{3(\gamma + 1)M_0^2}$ to the wall at $x = 0$, [c.f. (12)],

$$\begin{aligned} \frac{\partial k}{\partial \psi} &\simeq \frac{1}{(M_0^2 - 1)^{\frac{1}{2}}} \frac{\partial k}{\partial y} \quad \text{by (17)} \\ &= \frac{2(M_0^2 - 1)}{3(\gamma + 1)M_0^2} \frac{\partial k}{\partial x} = - \frac{2(M_0^2 - 1)N}{9(\gamma + 1)M_0^2(1 + A)} \quad \text{by (36)}. \end{aligned}$$

Hence
$$\frac{\partial k}{\partial y} = - \frac{2(M_0^2 - 1)^2 M_{SO}^2}{9(\gamma + 1)M_0^4(1 - M_{SO}^2)(1 + A)t_0} \quad \text{by (37).}$$

But/

But from (27), (36), and (17)

$$\frac{\partial^2 k}{\partial y^2} = \frac{2(M_0^2 - 1)^2 M_{SO}^4}{9M_0^4 (1 - M_{SO}^2)^2 (1 + A)^2 t_0^2} \text{ at } x = \psi = 0.$$

Thus there is no need for $\partial^3 k / \partial y^3$ to be infinite. Nevertheless, it remains true that at $x = \psi = 0$, $\partial k / \partial (N\psi)$ is much smaller than at most other points in the external flow (except where the flow is parallel to the wall), and $\partial^3 k / \partial (N\psi)^3$ and higher derivatives with respect to $N\psi$ are exceptionally large in magnitude; this choice of independent variable is pertinent because according to the next section, 3.6, k is a function only of A , Nx , $N\psi$, and the height of the channel.

The fact that the channel is assumed to be of constant height imposes an integral condition, as follows. If the centre line of the channel is the streamline $\psi = C$, and its distance from the wall is y_C , it follows from (17) that

$$y_C = t + \int_0^C \frac{\rho_0 u_0}{(M_0^2 - 1)^{1/2} \rho u} d\psi.$$

Hence from (34) and (25), approximately,

$$y_C = t_0 + \frac{2(M_0^2 - 1)(1 - M_{SO}^2) t_0}{(\gamma + 1) M_{SO}^2} [1 - k_S + A(1 - k_S)^2] + \frac{C}{(M_0^2 - 1)^{1/2}} - \frac{2(M_0^2 - 1)^{3/2}}{(\gamma + 1) M_0^2} \int_0^C k(1 - k) d\psi \dots (39)$$

Hence since $k = 1$ far upstream,

$$1 - k_S + A(1 - k_S)^2 = N \int_0^C k(1 - k) d\psi \dots (40)$$

Far downstream the pressure must be uniform across the channel, so that k must asymptote to its final value k_F everywhere. In other words,

$$k \rightarrow k_F \text{ as } x \rightarrow \infty \dots (41)$$

and from (40),
$$NC = \frac{1 + A(1 - k_F)}{k_F} \dots (42)$$

From the equation of motion (27) it can be seen that

$$\frac{\partial^2}{\partial x^2} [k(1 - k)] = - \frac{\partial^2 k}{\partial \psi^2}.$$

Hence (40) can be written

$$\frac{\partial^2}{\partial x^2} [1 - k_S + A(1 - k_S)^2] + N \left[\left(\frac{\partial k}{\partial \psi} \right)_{\psi=C} - \left(\frac{\partial k}{\partial \psi} \right)_{\psi=0} \right] = 0.$$

This is equivalent to (38), since

$$\frac{\partial k}{\partial \psi} = 0 \text{ at } \psi = C, \dots (43)$$

by/

by symmetry. Thus provided the boundary conditions (38), (41), (42), and (43) are satisfied, (40) will also be satisfied, so it need not be separately considered. It is worth noting too that symmetry requires

$$\frac{\partial^3 k}{\partial \psi^3} = \frac{\partial^5 k}{\partial \psi^5} = \dots = \frac{\partial^{2n+1} k}{\partial \psi^{2n+1}} = \dots = 0$$

on the centre line, in addition to (43), but these additional conditions are automatically met provided (43) is satisfied, when they follow from successive differentiations of the equation of motion (27).

3.6 The form of the solution downstream of the shock, and its rough evaluation

The equation of motion (27) has to be satisfied under the conditions, described in section 3.4, imposed by the shock, and under the further boundary conditions (38), (41), (42), and (43). Write $Nx = \bar{x}$, $N\psi = \bar{\psi}$, and $NX = \bar{X}$. Equation (27) becomes

$$\frac{\partial^2 k}{\partial \bar{\psi}^2} + \frac{\partial^2 k}{\partial \bar{x}^2} = \frac{\partial^2 k^2}{\partial \bar{x}^2}, \quad \dots (27')$$

and the relations (23), (26), (29), (30), (38), (41), (42) and (43) can be written as

$$\frac{(\gamma+1)M_0^2}{2} \frac{\partial m}{\partial \bar{x}} = \frac{\partial k}{\partial \bar{\psi}}, \quad \dots (23')$$

$$\frac{(\gamma+1)M_0^2}{2} \frac{\partial m}{\partial \bar{\psi}} = - \frac{\partial}{\partial \bar{x}} (k - k^2), \quad \dots (26')$$

$$\frac{(\gamma+1)M_0^2}{2} m_2 = \frac{1}{3} [1 - (2k_1 - 1)^{\frac{3}{2}}] + (k_1 + k_2 - 1)^{\frac{1}{2}} (k_1 - k_2), \quad \dots (29')$$

$$\frac{d\bar{X}}{d\bar{\psi}} = (k_1 + k_2 - 1)^{\frac{1}{2}}, \quad \dots (30')$$

$$[1 + 2A(1 - k)] \frac{\partial^2 k}{\partial \bar{x}^2} - 2A \left(\frac{\partial k}{\partial \bar{x}} \right)^2 + \frac{\partial k}{\partial \bar{\psi}} = 0 \text{ at } \bar{\psi} = 0, \quad \dots (38')$$

$$k \rightarrow k_F \text{ as } \bar{x} \rightarrow \infty, \quad \dots (41')$$

$$NC = \frac{1+A(1-k_F)}{k_F}, \quad \dots (42)$$

and $\frac{\partial k}{\partial \bar{\psi}} = 0 \text{ at } \bar{\psi} = NC. \quad \dots (43')$

Clearly, therefore, k is a function only of \bar{x} , $\bar{\psi}$, A , and k_F , whilst \bar{X} (defining the position of the shock) is a function only of $\bar{\psi}$, A , and k_F .

The upstream solution for k has already been given in section 3.5. Consider conditions a long way downstream, and write

$$k = k_F + k'.$$

Equation (27') becomes

$$\frac{\partial^2 k}{\partial \bar{\psi}^2} + \frac{\partial^2 k}{\partial \bar{x}^2} = 2(k_F + k') \frac{\partial^2 k}{\partial \bar{x}^2} + \left(\frac{\partial k}{\partial \bar{x}} \right)^2,$$

and far downstream it must approximate to

$$\frac{\partial^2 k}{\partial \bar{\psi}^2} + (1 - 2k_F) \frac{\partial^2 k}{\partial \bar{x}^2} = 0. \quad \dots(44)$$

This is because $\left(\frac{\partial k}{\partial \bar{x}} \right)^2$ must become very small compared with $\frac{\partial^2 k}{\partial \bar{x}^2}$; if the two terms were of the same order, k' would need to be proportional to $\log \bar{x}$, which is incompatible with (41'). Similarly the boundary condition (38') approximates downstream to

$$[1 + 2A(1 - k_F)] \frac{\partial^2 k}{\partial \bar{x}^2} + \frac{\partial k}{\partial \bar{\psi}} = 0 \text{ at } \bar{\psi} = 0. \quad \dots(45)$$

The solution of (44), under the boundary conditions (45), (41'), (42), and (43'), is

$$k = k_F + \alpha_1 \cos(B_1 S) e^{-B_1 \bar{x}} + \alpha_2 \cos(B_2 S) e^{-B_2 \bar{x}} + \dots$$

$$+ \alpha_r \cos(B_r S) e^{-B_r \bar{x}} + \dots$$

where
$$S \equiv (1 - 2k_F)^{\frac{1}{2}} \left\{ \frac{1 + A(1 - k_F)}{k_F} - \bar{\psi} \right\}$$

and for integral positive values of r

$$B_r (1 - 2k_F)^{\frac{1}{2}} \frac{[1 + A(1 - k_F)]}{k_F} = r\pi - \phi_r, \quad 0 < \phi_r < \frac{\pi}{2},$$

and
$$\tan \phi_r = \frac{B_r [1 + 2A(1 - k_F)]}{(1 - 2k_F)^{\frac{1}{2}}}.$$

} \dots(46)

If k_F is sufficiently small, $B_r \simeq \frac{r\pi k_F}{1 + A}$, and even when k_F is as large as 0.25, B_2 is roughly equal to $2B_1$.

The asymptotic solution (46) may be made the basis of a solution of the full equation (27'). Thus we may write

$$k = k_F + \alpha_1 \cos(B_1 S) e^{-B_1 \bar{x}} + \alpha_2 \cos(B_2 S) e^{-B_2 \bar{x}} + \alpha_3 \cos(B_3 S) e^{-B_3 \bar{x}} + \dots$$

$$+ g(\bar{\psi}) e^{-2B_1 \bar{x}} + h(\bar{\psi}) e^{-(B_1 + B_2) \bar{x}} + i(\bar{\psi}) e^{-3B_1 \bar{x}} + \dots \quad \dots(47)$$

where the equation (27') and the boundary conditions (38'), (41'), (42), and (43') will determine the functions g, h, i , etc., in terms of the arbitrary coefficients $\alpha_1, \alpha_2, \alpha_3$, etc. We thus obtain a solution with an infinite number of arbitrary coefficients, which can be found from the conditions imposed by the shock, (29') and (30'), in conjunction with (23') and (26'). The singularity at $\bar{x} = \bar{\psi} = 0$, mentioned in the preceding section, might give rise to some difficulty, but, in principle at any rate,

a solution in the form (47) is clearly possible. The functions h, i, etc., are tedious to evaluate, but g can be obtained relatively easily as follows. By substituting (47) in (27') and considering coefficients of $e^{-B_1 \bar{x}}$, $e^{-B_2 \bar{x}}$, and $e^{-2B_1 \bar{x}}$, we obtain, respectively, two relations which are identically satisfied, and a third relation,

$$4B_1^2(1 - 2k_F)g + \frac{d^2 g}{d\bar{\psi}^2} = 4B_1^2 \alpha_1^2 \cos^2(B_1 S). \quad \dots(48)$$

The boundary conditions (42) and (43') require

$$\frac{dg}{d\bar{\psi}} = 0 \text{ at } \bar{\psi} = \frac{1+A(1-k_F)}{k_F}. \quad \dots(49)$$

The boundary condition (38') yields equations, which are satisfied by (46), for the coefficients of $e^{-B_1 \bar{x}}$ and $e^{-B_2 \bar{x}}$, and a third equation for the coefficient of $e^{-2B_1 \bar{x}}$, viz.,

$$4B_1^2[1 + 2A(1 - k_F)]g + \frac{dg}{d\bar{\psi}} = 4AB_1^2 \alpha_1^2 \cos^2(B_1 S) \text{ at } \bar{\psi} = 0. \quad \dots(50)$$

The solution of Equations (48) to (50) is

$$g = \frac{\alpha_1^2}{2(1-2k_F)} + \beta \cos(2B_1 S) + \frac{B_1 \alpha_1^2}{2(1-2k_F)^{\frac{1}{2}}} \left[\frac{1+A(1-k_F)}{k_F} - \bar{\psi} \right] \sin(2B_1 S)$$

where $\frac{\beta}{\alpha_1^2} \{ 2(1 - 2k_F)^{\frac{1}{2}} \sin(2B_1 S_Z) + 4B_1 [1 + 2A(1 - k_F)] \cos(2B_1 S_Z) \}$

$$= 2AB_1 - \frac{2B_1 [1+2A(1-k_F)]}{1-2k_F} + \left\{ 2AB_1 + \frac{B_1 [1+A(1-k_F)]}{k_F} \right\} \cos(2B_1 S_Z)$$

$$+ \left\{ \frac{1}{2(1-2k_F)^{\frac{1}{2}}} - \frac{2B_1^2 [1+A(1-k_F)] [1+2A(1-k_F)]}{k_F (1-2k_F)^{\frac{1}{2}}} \right\} \sin(2B_1 S_Z)$$

and $S_Z \equiv S \text{ at } \bar{\psi} = 0.$

... (51)

The attached Table gives some values computed from (46) and (51) for B_1 , B_2 , and β/α_1^2 , and for $\cos(B_1 S)$, $\cos(B_2 S)$, and g/α_1^2 at $\bar{\psi} = 0$ and at $\bar{\psi} = nC$.

TABLE 4(a) A = 0

k_F	0.05	0.10	0.15	0.20	0.25	
B_1	0.157	0.314	0.471	0.635	0.810	
B_2	0.314	0.634	0.970	1.352	1.798	
β/α_1^2	-187	-19.7	-6.29	-2.92	-1.62	
$\bar{\psi} = 0$	$\cos(B_1 S)$	-0.987	-0.944	-0.872	-0.774	-0.657
	$\cos(B_2 S)$	0.949	0.816	0.652	0.505	0.366
	g/α_1^2	-177	-15.9	-4.17	-1.76	-1.05
$\bar{\psi} = nC$	$\cos(B_1 S)$	1	1	1	1	1
	$\cos(B_2 S)$	1	1	1	1	1
	g/α_1^2	-187	-19.1	-5.58	-2.09	-0.62

TABLE 4(b)/

TABLE 4(b) $k_F = 0.15$

A	0	0.4	0.8	1.2	
B_1	0.471	0.341	0.267	0.217	
B_2	0.970	0.713	0.563	0.465	
β/α_1^2	-6.29	-4.36	-3.69	-3.18	
$\bar{\psi} = 0$	$\cos(B_1 S)$	-0.872	-0.826	-0.800	-0.782
	$\cos(B_2 S)$	0.652	0.574	0.533	0.509
	g/α_1^2	-4.17	-2.57	-2.04	-1.70
$\bar{\psi} = nC$	$\cos(B_1 S)$	1	1	1	1
	$\cos(B_2 S)$	1	1	1	1
	g/α_1^2	-5.58	-3.65	-2.98	-2.47

It will be noticed that g/α_1^2 becomes very large for small values of k_F . This is not surprising because the exponential terms in the asymptotic solution (46) then decay very slowly, and (46) loses its usefulness as the basis for a solution in the form (47).

A very rough estimate of the magnitude of the coefficients α_1 and α_2 , and of the pressure distribution at the wall, can be made by assuming that k can be represented by

$$k = k_F + \alpha_1 \cos(B_1 S) e^{-B_1 \bar{x}} + \alpha_2 \cos(B_2 S) e^{-B_2 \bar{x}} + g(\bar{\psi}) e^{-2B_1 \bar{x}} \dots (52)$$

right up to the shock. Since B_2 is roughly equal to $2B_1$, it is appropriate to neglect the terms in (47) involving α_2 , etc., if the terms involving h , i , etc., are neglected also. Equation (52) involves two unknowns, α_1 and α_2 , since g can be found as above in terms of α_1^2 . The unknowns α_1 and α_2 can be found by imposing the conditions that

$$k = \frac{1}{2} \text{ at } x = \bar{\psi} = 0, \dots (53)$$

and that $k = 0$ on the centre line immediately behind the shock. [c.f. section 3.1.] The shock in the centre is some way to the right of the line $x = 0$. [c.f. Fig. 3.] From Equation (30') we see that the maximum possible value of $d\bar{x}/d\bar{\psi}$ would occur with the maximum possible values of k_1 and k_2 , and since $1 \geq k_1 \geq \frac{1}{2}$ and $\frac{1}{2} \geq k_2 \geq 0$, the maximum possible value of $d\bar{x}/d\bar{\psi}$ is $1/\sqrt{2}$. Probably however the actual maximum value of $d\bar{x}/d\bar{\psi}$, which will occur somewhere between $\bar{\psi} = 0$ and the centre line $\bar{\psi} = nC$, will be in the region of $\frac{1}{2}$. Since $d\bar{x}/d\bar{\psi} = 0$ both at $\bar{\psi} = 0$ and $\bar{\psi} = nC$, it is reasonable to assume that the average value of $d\bar{x}/d\bar{\psi}$ is in the region of $1/8$, so that on the

centre line $\bar{x} = \frac{nC}{8} = \frac{1+A(1-k_F)}{8k_F}$ by (42). Thus the condition that

$k = 0$ immediately behind the shock on the centre line is roughly equivalent to

$$k = 0 \text{ at } \bar{x} = \frac{1+A(1-k_F)}{8k_F}, \bar{\psi} = \frac{1+A(1-k_F)}{k_F}. \dots (54)$$

Conditions (53) and (54) applied to (52) determine a very rough solution. Computed values are given in the Table.

TABLE 5(a)/

TABLE 5(a) A = 0

k_F	0.05	0.10	0.15	0.20	0.25
α_1	-0.231	-0.275	-0.343	-0.412	-0.632
α_2	10.20	1.64	0.830	0.555	0.694

\bar{x}	0	1	2	3	4	5	6	7	8	9	10
k at $\bar{\psi}=0$ for $k_F=0.05$	0.50	0.41	0.34	0.28	0.24	0.20	0.17	0.15	0.13	0.12	0.11
0.10	0.50	0.36	0.28	0.22	0.18	0.16	0.14	0.13			
0.15	0.50	0.35	0.27	0.22	0.20	0.18					
0.20	0.50	0.36	0.29	0.25	0.22						
0.25	0.50	0.39	0.32	0.28	0.27						

TABLE 5(b) $k_F = 0.15$

A	0	0.4	0.8	1.2
α_1	-0.343	-0.348	-0.358	-0.370
α_2	0.830	0.652	0.609	0.578

\bar{x}	0	1	2	3	4	5	6	7	8	9	10
k at $\bar{\psi}=0$ for A=0	0.50	0.35	0.27	0.22	0.20	0.18					
0.4	0.50	0.38	0.31	0.26	0.23	0.20	0.19	0.18			
0.8	0.50	0.40	0.33	0.29	0.25	0.23	0.21	0.19	0.18	0.18	
1.2	0.50	0.42	0.35	0.31	0.28	0.25	0.23	0.21	0.20	0.19	0.18

These values for k at $\bar{\psi} = 0$, together with the values for the upstream solution given in Table 3 of section 3.5, are plotted against \bar{x} in Figs. 6 and 7. It can be seen that in all cases the pressure gradients tend to be a good deal less steep downstream of the shock, where the external flow is subsonic, than they are just upstream of the shock. It is, of course, not certain that the accurate solution for the flow downstream of the shock would behave like this. The solution in the form (52) is very crude, and it would be desirable to consider many more terms of the complete solution (47). However, the practical difficulty of working out the terms h , i , etc., would make this very laborious. The expression (52) in effect extrapolates up to the shock a form of solution which is valid at large values of \bar{x} . This procedure is perhaps to some extent justified by the fact that the terms in α_2 and g in (52) tend to cancel one another. Hence the solution for k at $\bar{\psi} = 0$ would not be vastly different if it were simply assumed that $\alpha_2 = g = 0$ in (52), and the single condition (53) were applied to find α_1 . Thus it is at any rate plausible to suppose that the full solution of the problem would agree qualitatively with Figs. 6 and 7.

4. The Application of the Solution to the Problem of the Interaction of a Weak Normal Shock with a Turbulent Boundary Layer

As was pointed out in the Introduction, it is not to be expected that the simple model studied above should give results in close quantitative agreement with experiment. The most important factor neglected by the theory is turbulent friction. Even apart from this, however, there is no clear-cut relationship between the model shown in Fig. 1 of a uniform subsonic layer, and the real turbulent boundary layer profile. The initial Mach number M_{SO} and thickness t_0 of the subsonic layer must be chosen so as to give what may be regarded as the best representation of the real profile, but such a choice is, within limits, arbitrary. Since the solution depends on M_{SO} and t_0 insofar as it depends on

$$N = \frac{M_{SO}^2 (M_0^2 - 1)^{\frac{1}{2}}}{M_0^2 (1 - M_{SO}^2) t_0},$$

it/

it is plausible to choose M_{SO} and t_0 such that

$$\frac{(1-M_{SO}^2)Y}{M_{SO}^2} = \int_0^Y \frac{(1-M^2)}{M^2} dy \quad \text{and} \quad t_0 = FY,$$

where $M(y)$ is the Mach number in the undisturbed turbulent layer upstream of the region of interaction at a distance y from the wall, Y is the thickness of the subsonic part of the layer, so that $M(Y) = 1$, and F is some fraction of order 1. If we assume that the velocity distribution in the undisturbed turbulent boundary layer can be represented by

$$\frac{u}{u_0} = \left(\frac{y}{\delta} \right)^{\frac{1}{7}},$$

where u_0 is the velocity outside the boundary layer and δ is its total thickness, we have for the case of zero heat transfer, where it can be assumed that the total temperature is constant across the layer,

$$\left(\frac{u}{u_0} \right)^2 = \frac{M^2 (1 + \frac{Y-1}{2} M_0^2)}{M_0^2 (1 + \frac{Y-1}{2} M^2)} = \left(\frac{y}{\delta} \right)^{\frac{2}{7}}.$$

It follows that for $\gamma = 1.4$

$$\frac{1-M^2}{M^2} = \frac{1}{5} \left(\frac{5}{M_0^2} + 1 \right) \left(\frac{y}{\delta} \right)^{-\frac{2}{7}} - \frac{6}{5}.$$

Thus the thickness Y of the subsonic part of the layer is given by

$$\frac{Y}{\delta} = \left[\frac{1}{6} \left(\frac{5}{M_0^2} + 1 \right) \right]^{\frac{7}{2}} = \frac{t_0}{F\delta},$$

and

$$\frac{1-M_{SO}^2}{M_{SO}^2} = \frac{1}{Y} \int_0^Y \frac{(1-M^2)}{M^2} dy = \frac{12}{25}.$$

Hence $M_{SO} = 0.822$. The constant A can thus be determined as a function of M_0 by interpolation from Table 1 of section 3.5, and it is given together with $t_0/F\delta$ in Table 6 below. Values of $1/FN\delta$ are also included in this Table, enabling the independent variable \bar{x} of the solution to be converted to a physical distance. Thus $\bar{x} = Nx$ so that

$\frac{x}{\delta} = \frac{F\bar{x}}{FN\delta}$. Finally the ratio of the half-height y_c of the channel to

the boundary-layer thickness δ has been computed from Equations (39), (40), and (42) and presented in Table 6 as a function of the final downstream value of k , k_F : the relation for $y_c/F\delta$ is

$$\frac{y_c}{F\delta} = \frac{t_0}{F\delta} \left[1 + \frac{NC}{t_0(M_0^2-1)^{\frac{1}{2}}N} \right] = \frac{t_0}{F\delta} \left[1 + \frac{12[1+A(1-k_F)]M_0^2}{25k_F(M_0^2-1)} \right].$$

TABLE 6/

TABLE 6

M ₀	1	1.02	1.04	1.06	1.08	1.10
A	0	0.18	0.35	0.56	0.83	1.2
$t_c/F\delta = Y/\delta$	1	0.89	0.79	0.72	0.64	0.58
$1/FN\delta$	∞	2.49	1.44	1.11	0.88	0.74
$y_c/F\delta$ for $k_F=0.05$	∞	259	134	97	77	70
0.10	∞	130	67	48	38	34
0.15	∞	85	44	32	25	22
0.20	∞	64	33	24	19	16
0.25	∞	51	26	19	15	13

For a section of the channel of width ω , the cross-sectional area of the boundary layers on both walls is $2\omega\delta$, whilst the cross section of the channel is $2y_c\omega$, so that the ratio is δ/y_c . If we consider the flow in a circular pipe of radius r , the cross-sectional area of the boundary layer round the pipe circumference is $2\pi r\delta$, whilst the area of the pipe is πr^2 , so that the ratio is $2\delta/r$. Hence for a weak normal shock in a circular pipe r/δ needs to be twice as large as y_c/δ as given in Table 6 to give the same final downstream pressure.

The ratio of the overall increase of pressure through the shock to the increase of pressure that would in theory occur in the absence of a boundary layer is equal to $1 - k_F$. Hence it is evident from Table 6 that in any experiment with normal shocks in a channel or pipe the boundary layer must be very thin compared with the channel height or pipe diameter if a large fraction of the theoretical inviscid pressure rise is to be achieved with an initial Mach number M_0 near 1. This makes the experiment a rather difficult one because it is desirable to have as thick a boundary layer as possible for the measurement of pressure distributions, velocity profiles, etc. It is probably partly because of this difficulty that no such experiment has been performed to date. The results of the theory can in certain respects be compared with experimental results obtained in transonic flow past, for example, an aerofoil. However the surface is usually curved in such a case, and the upstream supersonic flow is certainly not uniform, so that there are important differences from the case of a shock in a straight channel or pipe. Thus, as Ackeret, Feldman, and Rott² and Emmons³ have shown, surface curvature would, even in the absence of a boundary layer, be expected to give rise to a singularity at the shock with a reduced downstream pressure. Probably, however, in the presence of a boundary layer, the relatively steep pressure gradients that occur where the external flow is supersonic would be little affected by surface curvature or by lack of uniformity in the upstream flow. Thus the maximum pressure gradient under the shock should depend only on the external-flow Mach number M_0 just upstream of the shock near the wall and on the thickness of the boundary layer.

According to our solution, the pressure gradient at the wall at $x = 0$, where the supersonic region terminates, is close to the maximum gradient. [See Figs. 6 and 7.] At $x = \psi = 0$, where $k = k_S = \frac{1}{2}$, Equation (36) shows that

$$\frac{dk_S}{dx} = \frac{N}{3(1+A)}$$

This means that the maximum pressure gradient at the wall is given by

$$\delta \frac{d}{dx} \left(\frac{p}{p_0} \right) \approx \frac{2\gamma}{\gamma+1} \frac{(M_0^2-1)N\delta}{3(1+A)} = 0.39 \frac{(M_0^2-1)N\delta}{1+A}$$

if $\gamma = 1.4$. In terms of the stagnation pressure H

$$\delta \frac{d}{dx} \left(\frac{p}{H} \right) = \frac{0.39(M_0^2 - 1)N\delta}{(1+A)(1 + \frac{M_0^2}{5})^{3.5}}$$

Values have been computed from Table 6 as functions of M_0 , and are as follows:

TABLE 7

M_0	1	1.02	1.04	1.06	1.08	1.10
Maximum values of $F\delta \frac{d}{dx} \left(\frac{p}{p_0} \right)$	0	0.005	0.016	0.028	0.040	0.050
Maximum values of $F\delta \frac{d}{dx} \left(\frac{p}{H} \right)$	0	0.003	0.008	0.014	0.019	0.023

Experimental results⁷ obtained from a two-dimensional curved surface attached to the wall of a subsonic wind tunnel are shown in Fig.8. The figure shows a family of pressure distributions in the neighbourhood of the nearly-normal shock for various free-stream Mach numbers. The thickness δ of the turbulent boundary layer was about 0.35", so that for the weakest shock, for which $M_0 = 1.14$,

$\delta \frac{d}{dx} \left(\frac{p}{H} \right) \approx 0.08$. The values of Table 7, extrapolated to $M_0 = 1.14$, suggest that at that Mach number, $F\delta \frac{d}{dx} \left(\frac{p}{H} \right) \approx 0.028$. Thus to obtain

agreement with experiment we need to assume $F \approx 0.35$. This seems at first sight rather small, since the most obvious assumption is that t_0 , the thickness of the subsonic layer in the model of Fig.1, is equal to Y , the thickness of the subsonic part of the real layer. Thus one might reasonably suppose that a value of F quite near 1 would take care of any errors arising from the somewhat arbitrary choice of M_{S0} and t_0 . The smaller value of F , however, probably compensates in a rough and ready way for the neglect of turbulent friction effects in the theory. Equation (34) for the thickness t of the subsonic layer may be written

$$t - t_0 = \frac{2(M_0^2 - 1)(1 - M_{S0}^2)t_0}{(\gamma + 1)M_{S0}^2} [1 - k_S + A(1 - k_S)^2], \quad \dots(34')$$

and the left hand side of this equation is equated with the amount by which the innermost streamline of the external flow is displaced outwards from its original distance from the wall. This displacement is probably overestimated by (34') if t_0 is put equal to Y on the right hand side, because (34') is based on the assumption of frictionless flow. In reality, because of friction, the subsonic flow is not slowed down by increasing pressure as much as is assumed, and hence the stream-tube areas do not increase as much. This makes it understandable that the best agreement with experiment should apparently be obtained with $F \approx 0.35$. However more detailed comparison with experiment is desirable to determine whether or not the value $F = 0.35$ brings roughly into line with experiment the other predictions of the theory, such as the relationship given in Table 6 between y_c , the half-height of the channel, and M_0 and k_F .

The distributions of Fig.8 show that the pressure gradient under the shock increases at first with increasing Mach number M_0 for values of M_0 near 1, where M_0 corresponds to the minimum pressure at the surface of the aerofoil just upstream of the shock. However the gradient tends to an approximately constant limit for rather higher values of M_0 . The results of Table 7 appear to be consistent with this.

It is interesting to note that the solution indicates that as the Mach number M_0 approaches 1, the region of upstream influence of the shock increases, despite the fact that the pressure rise through the shock decreases. This apparently paradoxical result is due to the fact that the thickening of the subsonic layer tends to be proportional to the pressure rise, and hence to $(M_0^2 - 1)$, whilst the maximum deflection of the external flow from its free stream direction is proportional to $(M_0^2 - 1)^{\frac{3}{2}}$. To accommodate the increase in boundary layer thickness, therefore, the region of upstream influence tends to vary as $(M_0^2 - 1)^{-\frac{1}{2}}$. This effect is, however, only operative at Mach numbers close to 1, because of the non-linear relation between pressure and the thickness of the subsonic layer.

It may be desired to obtain a rough estimate of the overall increase $\Delta\delta^*$ in boundary-layer displacement thickness through the shock wave. The left hand side of Equation (34'), $(t - t_0)$, may be put equal to $\Delta\delta^*$, and assuming $M_{S0} = 0.822$, $\gamma = 1.4$, and, tentatively, $t_0 = 0.35Y$, we obtain

$$\frac{\Delta\delta^*}{\delta} = 0.14 (M_0^2 - 1) \frac{Y}{\delta} [1 - k_F + A(1 - k_F)^2],$$

where k_F , the final downstream value of k , depends on the dimensions of the channel, as in Table 6. For an infinite channel or pipe $k_F = 0$ and

$$\frac{\Delta\delta^*}{\delta} = 0.14 (M_0^2 - 1)(1 + A) \frac{Y}{\delta}.$$

Values of this expression computed from Table 6 are given in Table 8. The upstream value of the displacement thickness δ^* is approximately equal to 0.16δ for M_0 in the range 1 to 1.1, [c.f. Ref.8], and values of the proportional increase in δ^* , $\frac{\Delta\delta^*}{\delta^*}$, have also been included in the Table.

TABLE 8

M_0	1	1.02	1.04	1.06	1.08	1.10
$\frac{\Delta\delta^*}{\delta}$	0	0.006	0.012	0.019	0.027	0.038
$\frac{\Delta\delta^*}{\delta^*}$	0	0.04	0.08	0.12	0.17	0.24

The results of Table 8 are of course only tentative since it is only a possibility that by putting $t_0 = 0.35Y$ and $M_{S0} = 0.822$, as above, the behaviour of a real turbulent boundary layer can in all respects be approximately represented by the theoretical results for a uniform frictionless layer.

5. Conclusions

The solution obtained suggests that Figs. 6 and 7 represent the general shape of the pressure distributions at the wall for interactions between a weak normal shock wave in a straight channel and a turbulent boundary layer. However the following points must be borne in mind:-

(i) The model of a frictionless subsonic layer shown in Fig.1 is an artificial one, (a) because it ignores friction, and (b) because even

if friction played a negligible rôle in the real case, (except very near the wall where it is essential if flow reversal is to be avoided), the real profile is not the same shape as Fig.1.

(ii) Downstream of $\bar{x} = 0$ the accurate solution has not been found even for the simplified model of Fig.1.

With regard to this last point, there are reasonable grounds for believing that the accurate solution would be of the same general shape as shown in Figs. 6 and 7, at least to the extent that $(k - k_F)$ would be appreciable over about the same range of \bar{x} for both the accurate and approximate solutions. Point (i)(b) is also probably of fairly minor importance; if friction only played a negligible part in the real layer, except very near the wall, the solution for the model of Fig.1 would probably represent the behaviour of the real layer quite well with M_{S0} put equal to 0.822 and t_0 put equal to FY with F not far from 1. In reality, however, the effects of friction will not be confined to the laminar sublayer. If F is put equal to 0.35, the theoretical prediction for the maximum pressure gradient with $M_0 = 1.14$ can be made to agree with experiment. This somewhat low value of the factor F serves partly to account in a rough and ready way for friction effects, and it may be that, very crudely, putting $F = 0.35$ suffices to bring all the theoretical results quantitatively into line with experiment. Even if this does not prove to be the case, however, it seems quite possible that the results will still resemble qualitatively those that would be obtained with real turbulent layers.

Although the theoretical results have been obtained for the case of a straight two-dimensional channel, it is likely on physical grounds that there would be little difference with a pipe of circular cross section, provided that the radius of the pipe were related to the height of the corresponding channel as discussed in the preceding section. Hence the above remarks can be taken to apply to the flow in a pipe as well. Pipe flow is of course easier to achieve experimentally than two-dimensional channel flow.

To sum up: The theoretical results suggest that in experiments with upstream Mach numbers M_0 in the range 1 to 1.1, and with the dimensions of the pipe or channel adjusted so as to make the overall pressure rise a given fraction of the theoretical normal-shock value, the pressure distributions at the wall should not be too sensitive to M_0

when plotted in the form of $\frac{p-p_0}{(M_0^2-1)p_0}$ against $\frac{(M_0^2-1)^{\frac{1}{2}} x}{M_0^2(1+A)\frac{Y}{\delta}}$, where A

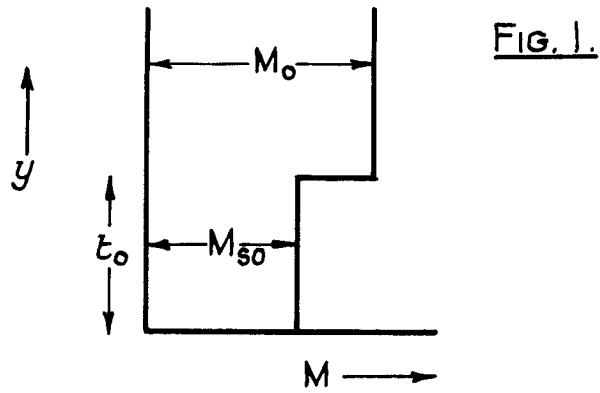
and Y/δ are given as functions of M_0 in Table 6, p is pressure, p_0 the upstream pressure, and δ the boundary-layer total thickness. If this method of correlating experimental results should prove fruitful, and the results resemble qualitatively those shown in Figs. 6 and 7, it would be reasonable to conclude that friction is not of dominant importance in the interaction, but that the frictionless "Bernouilli" thickening of the subsonic boundary-layer flow with increase of pressure is at least a very significant factor also.

References/

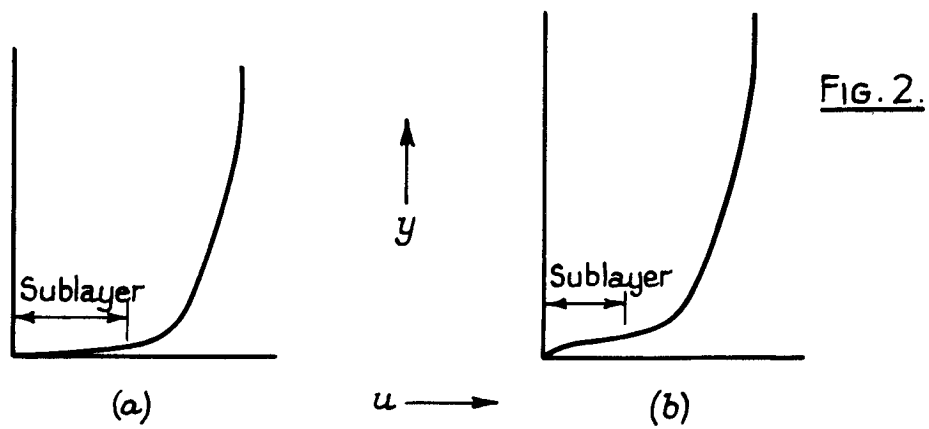
References

<u>No.</u>	<u>Author(s)</u>	<u>Title, etc.</u>
1	H. H. Pearcey	Some effects of shock-induced separation of turbulent boundary layers in transonic flow past aerofoils. Paper No.9 presented at the Symposium on Boundary Layer Effects in Aerodynamics, held at the N.P.L., March/April, 1955. London, H.M.S.O., 1955.
2	J. Ackeret, F. Feldmann, and N. Rott. (Translated by I. M. Davidson and G. Korbacher.)	Investigation on compression shocks and boundary layers in fast moving gases. (Institut für Aerodynamik, E.T.H. Zurich, Report No.10, 1946) A.R.C.10,044 - F.M.996.
3	H. W. Emmons	The theoretical flow of a frictionless, adiabatic, perfect gas inside of a two-dimensional hyperbolic nozzle. N.A.C.A. Tech. Note 1003, 1946.
4	D. W. Holder	Experiments on an aerofoil section designed to be free from shock-induced separation at all Mach numbers for small angles of incidence. In preparation.
5	H. S. Tsien and M. Finston	Interaction between parallel streams of subsonic and supersonic velocities. J.Aero.Sci., Vol.16, 1949, p.515.
6	M. J. Lighthill	On boundary layers and upstream influence. Part II. Supersonic flows without separation. Proc. Roy. Soc. A, Vol.217, 1953, p.478.
7	L. H. Tanner	Unpublished data obtained at N.P.L., 1955.
8	W. F. Cope	Notes and graphs for boundary layer calculations in compressible flow. C.P.89. August, 1951.

FIGS. 1 - 3.

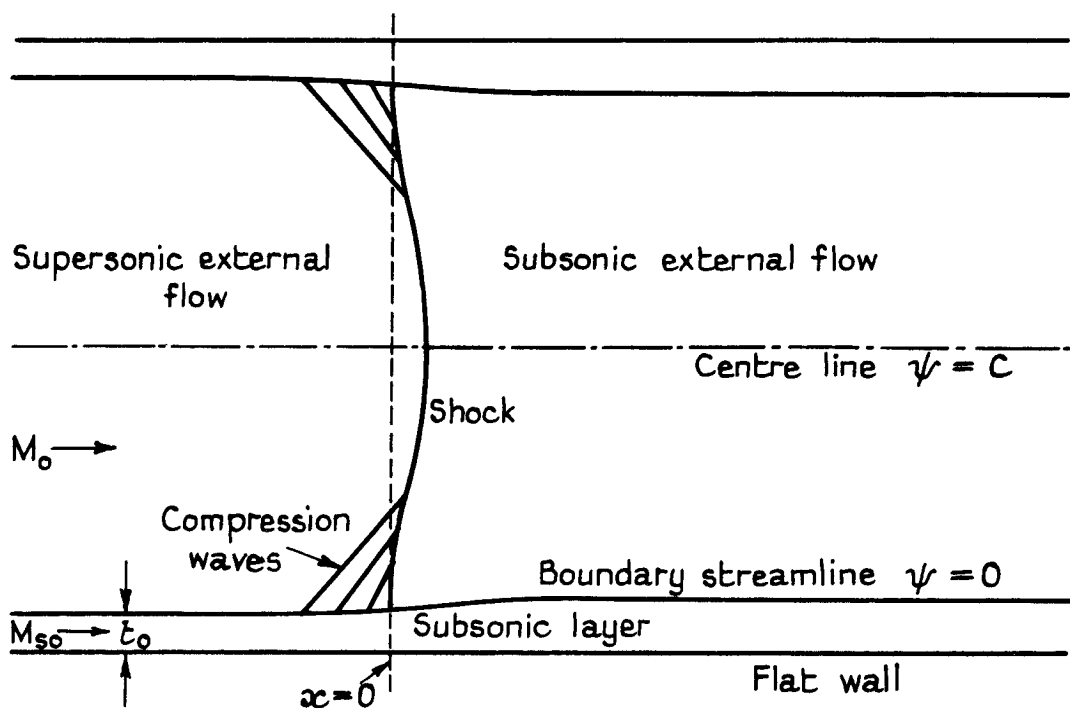


The idealized boundary-layer Mach-number profile



The shape of the real boundary-layer velocity profile, (a) upstream, and also, (b) after experiencing an increase of pressure.

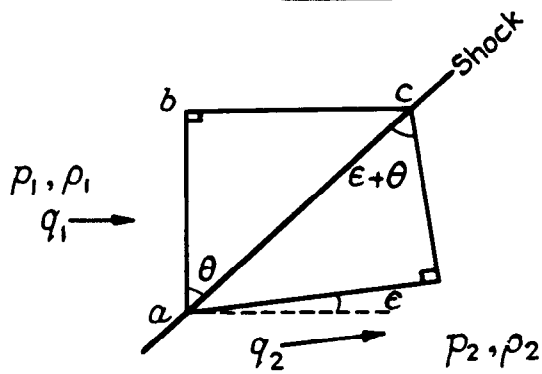
FIG. 3.



The overall flow pattern for the flow in a two-dimensional channel.

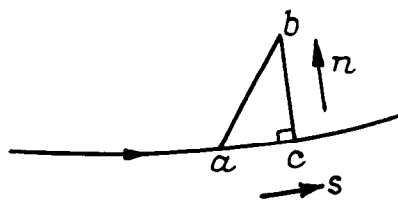
FIGS. 4 - 6.

FIG. 4.



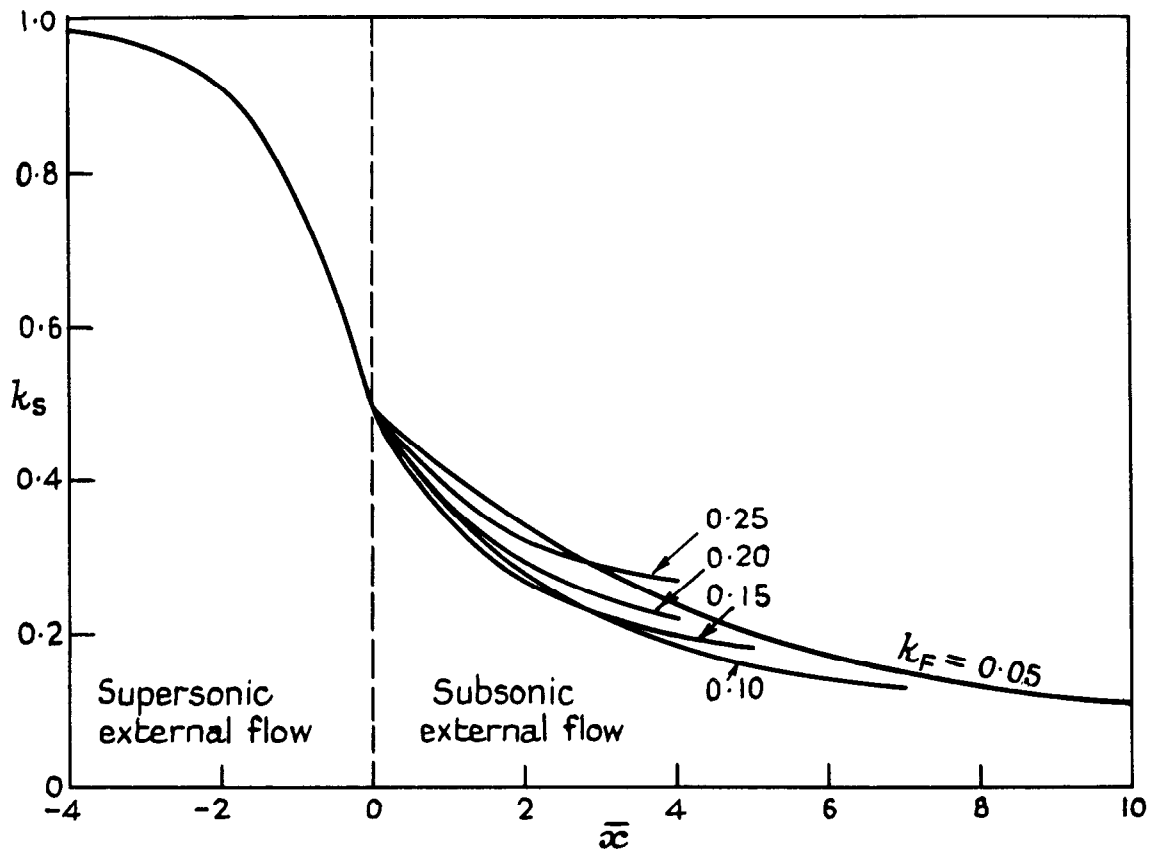
The flow through an oblique shock

FIG. 5.



A streamline in the simple - wave region

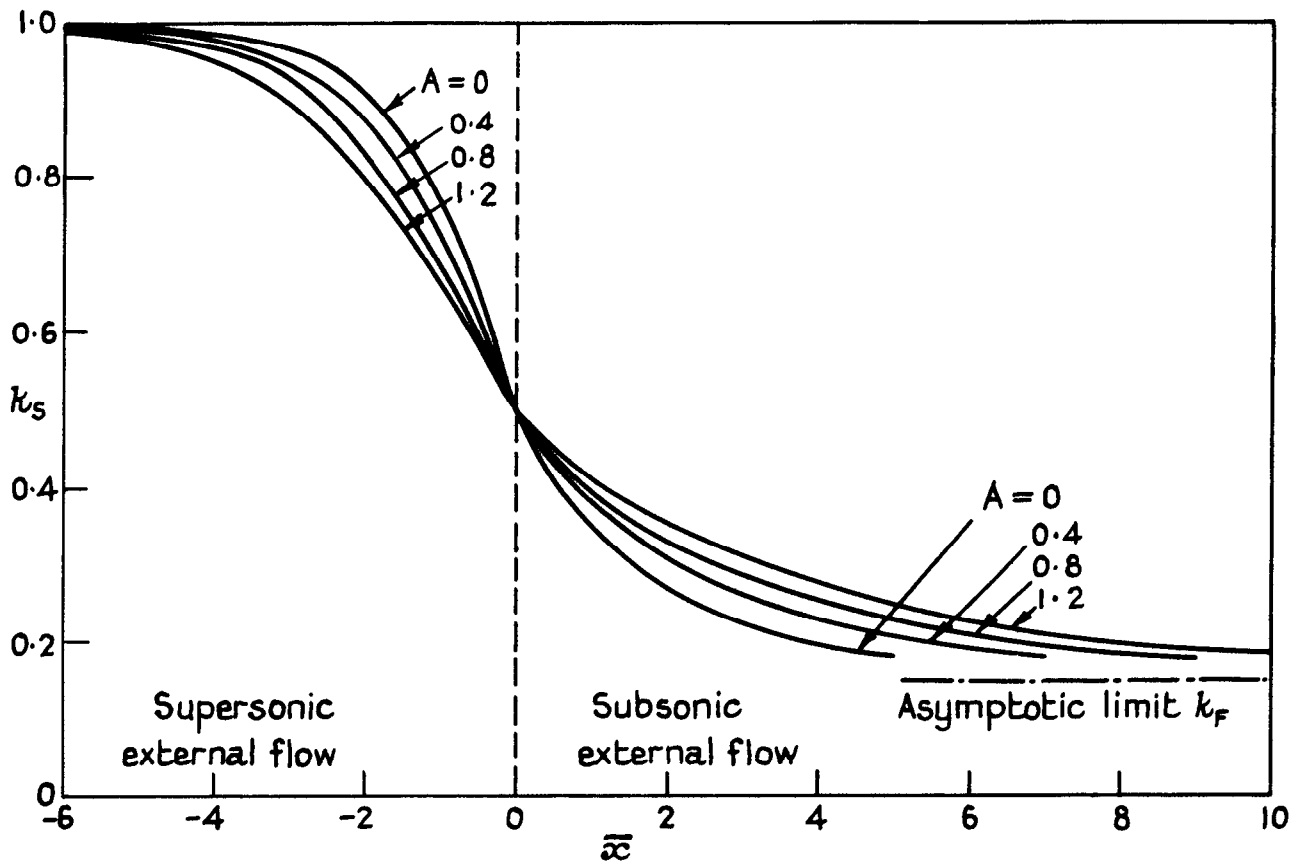
FIG. 6.



Computed distributions of k_s , equal to $1 - \frac{(\gamma+1)(p-p_0)}{2\gamma(M_0^2-1)p_0}$ at the wall,
as a function of \bar{x} , equal to $\frac{M_{s0}^2(M_0^2-1)^{1/2}\bar{x}}{M_0^2(1-M_{s0}^2)\bar{x}_0}$, for various values of
 k_F with A equal to 0

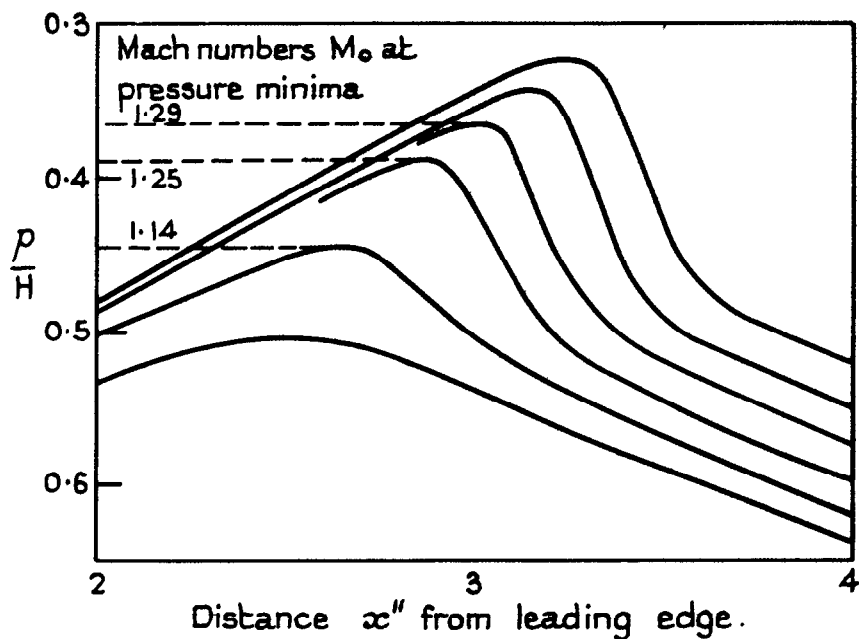
FIGS. 7 & 8.

FIG. 7.



Computed distributions of k_s , equal to $1 - \frac{(\gamma+1)(p-p_0)}{2\gamma(M_0^2-1)p_0}$ at the wall,
as a function of \bar{x} , equal to $\frac{M_{so}^2(M_0^2-1)^{1/2}\bar{x}}{M_0^2(1-M_{so}^2)t_0}$, for various values of
 A with $k_F = 0.15$.

FIG. 8.



Experimental pressure distributions on a bump
on a tunnel wall.

C.P. No. 424

(18,735)

A.R.C. Technical Report

© *Crown copyright 1959*

Printed and published by
HER MAJESTY'S STATIONERY OFFICE

To be purchased from
York House, Kingsway, London W.C.2
423 Oxford Street, London W.1
13A Castle Street, Edinburgh 2
109 St Mary Street, Cardiff
39 King Street, Manchester 2
Tower Lane, Bristol 1
2 Edmund Street, Birmingham 3
80 Chichester Street, Belfast
or through any bookseller

Printed in Great Britain

S.O. Code No. 23-9011-24

C.P. No. 424